

## **Properties of a Streamwise Turbulent Flow Field in an Open Two-Stage Channel**

**Paweł M. Rowiński\***, **Włodzimierz Czernuszenko\***, **Adam P. Koziol\*\***,  
**Janusz Kubrak\*\***

\* Institute of Geophysics, Polish Academy of Sciences, ul. Księcia Janusza 64,  
01–452 Warszawa, Poland

\*\* Faculty of Environmental Science, Warsaw Agriculture University SGGW,  
ul. Nowoursynowska 166, 02–787 Warsaw, Poland

(Received April 15, 2002; revised September 8, 2002)

### **Abstract**

The results of the experimental studies, aimed at the recognition of the streamwise turbulent structure in a compound channel, are reported in this paper. Three sets of measurements with electromagnetic liquid velocity meter were used: one in a smooth channel, one with the rough overbank channels and the last one with the modelled high vegetation occurring on floodplains. The analyses included vertical distributions of local mean velocities, depth-averaged mean velocities, bed shear stresses, turbulent intensities, higher order velocity moments, autocorrelation and velocity spectra. Relevant turbulent temporal and spatial scales were evaluated. All the properties were investigated with special emphasis placed on the influence of roughness on them.

### **1. Introduction**

Rivers during flood are characterized by a compound cross-section (water overflows the banks to floodplains) and unsteady flow. The characteristics of turbulence are not well recognized in such a situation. One may suspect that additional flow resistance occurs due to intensive momentum exchange between the deep main channel and the adjacent shallow floodplains. The flow structures that occur in rivers of a compound cross-section are very complex due to at least three mechanisms: boundary-generated turbulence, free shear layer turbulence and velocity fluctuations associated with perturbations in the longitudinal secondary flow cells (Shiono and Knight 1991, Tominaga and Nezu 1991). To make the considerations simpler, it is convenient to study the geometrical and temporal complexities separately, i.e. to study the turbulence structure in a compound cross-section at steady state conditions and to study turbulence under an unsteady state condition. The authors have been involved in the latter problem quite recently (Rowiński and

Czernuszenko 1998, Rowiński et al. 2000). The first problem will be discussed in the present study. Experimental investigations performed in a laboratory compound channel will be considered. Partial and preliminary results of this paper were reported by Rowiński et al. (1998).

Shallow floodplains occurring in nature are usually rough and a lot of attention has recently been paid to the investigations of the influence of various roughness conditions on the flow structure (e.g. Sofialdis and Prinos 1999, Knight and Brown 2000, Myers et al. 2000). The present paper goes along similar lines and its main goal consists in measuring and analysing the distribution of the main velocity component, bottom shear stress and the distribution of longitudinal turbulence characteristics in different hydraulic conditions. Although more sophisticated experimental methods pertaining to 3D flow structure become available, the longitudinal velocity data is still very often considered in literature discussing basic properties of turbulence in river flows (e.g. Barua and Rahman 1998, Dinehart 1999, Nikora et al. 1994, Nikora and Smart 1997, Smart 1999). The records in this study represent longitudinal velocities sampled from the sensor output at 2.5 Hz. It obviously precludes the analyses of eddies indicated by higher frequencies. Nevertheless the obtained data provide substantial information on the turbulent structure and studies at this level of accuracy are a frequent practice in worldwide research (e.g. Dinehart 1999).

Experiments were conducted in a trapezoidal straight open channel with symmetrically complex cross-section with inclined side-walls. Various hydraulic conditions were achieved by changing the roughness of floodplains, therefore, three series of experiments were performed – the first being carried out in a smooth concrete channel (both main channel and floodplains), the second was performed in a channel with floodplains covered by cement mortar composed with terrazzo and in the third test, plants (trees) growing on the floodplains were modelled by aluminium pipes placed on the floodplains. Studies of the turbulent structure in vegetated channels is rather scarce at the moment, but the importance of it is emphasized by many authors and some efforts in this respect have been undertaken recently (e.g. Nepf 1999, Nepf and Vivoni 2000, Nezu and Onitsuka 2001).

## 2. Experimental Procedure

The experiments considered herein were carried out in the Hydraulic Laboratory of the Department of Hydraulic Structures, Faculty of Environmental Science at the Warsaw Agricultural University. A straight open channel with symmetrically complex trapezoidal cross section, 16 m long and 2.10 m wide was used for the laboratory tests. The cross-section at half of the channel length was selected for measurements (Fig. 1). The bed slope of the channel was 0.0005 and the water surface was kept parallel to the bed during the experiments. Three tests for three various roughness of floodplains were realized. In the first experiment the channel

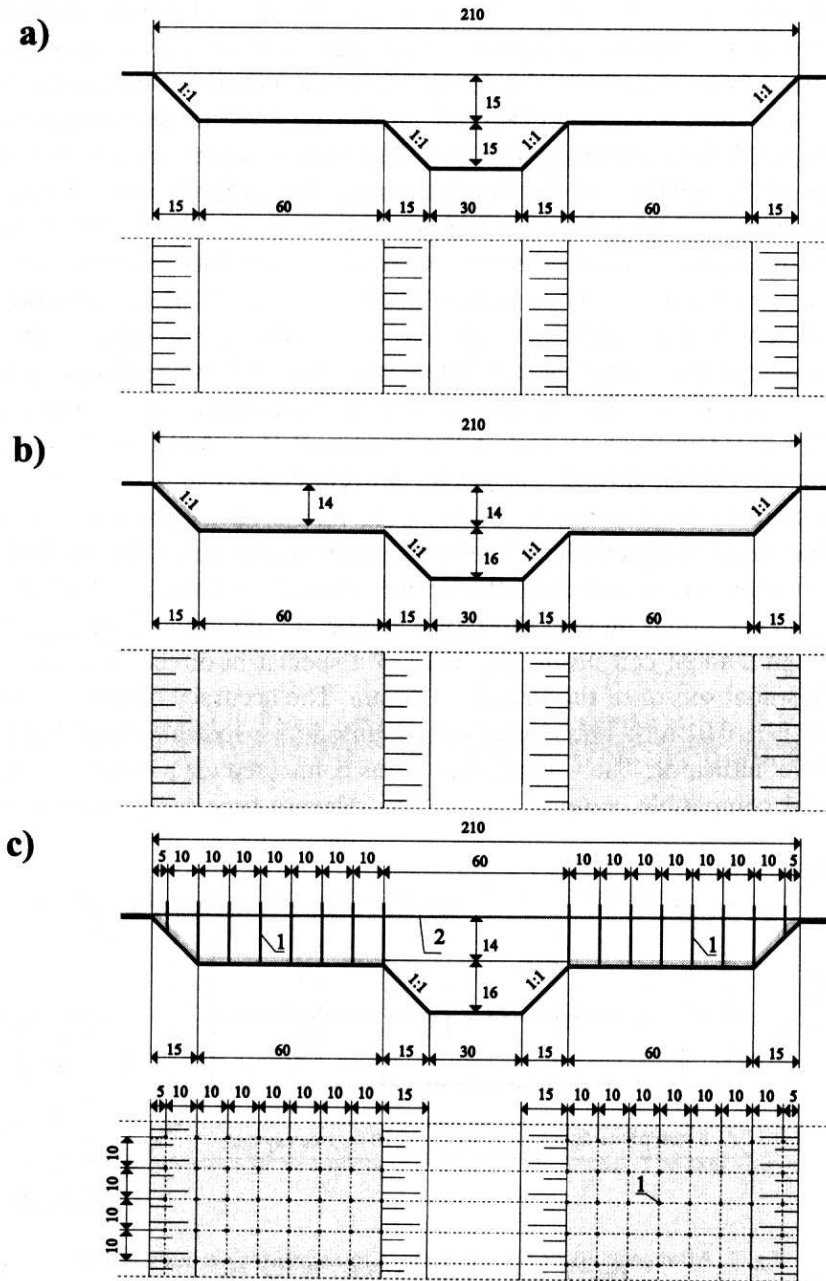


**Fig. 1.** Scheme of a laboratory cross-section for three considered tests:  
 a) test 1 in a smooth channel b) test 2 in a channel with rough floodplains,  
 c) test 3 in a channel with rough floodplains vegetated with trees

may be considered as a smooth one covered by concrete and characterized by Manning coefficient  $n = 0.010 \text{ m}^{-1/3} \text{ s}$ . In the second test the floodplains were covered by cement mortar composed of terrazzo (0.5 to 1 cm in diameter) and characterized by  $n = 0.018 \text{ m}^{-1/3} \text{ s}$ . More information on the roughness conditions in the given channel is given in (Kubrak 1999) where the dimensionless values of roughness coefficient appearing in Darcy-Weisbach resistant law are provided. In the third test the covering of the floodplains was left as in the second experiment but additionally high vegetation (trees) growing on the floodplains were modelled by aluminium pipes of 0.8 cm diameter, placed with both longitudinal and lateral spacings of 10 cm (Fig. 1). There were 16 pipes in each of 161 cross-sections. The stick-tops were above water level and the pipes were not subject to any elastic strains caused by overflowing water. The water level and the discharge in the first experiment was  $H = 0.202 \text{ m}$  and  $Q = 68.33 \text{ l/s}$  respectively, in the second –  $H = 0.219 \text{ m}$ ,  $Q = 50.36 \text{ l/s}$  and in the third one  $H = 0.212 \text{ m}$ ,  $Q = 38.92 \text{ l/s}$ . A uniform and steady flow was achieved in every case.

Instantaneous longitudinal velocities were measured with the use of the programmable electromagnetic liquid velocity meter manufactured by Delft Hydraulics. The principle of operation of the device is based on Faraday's Induction Law for a conductive liquid moving through a magnetic field induced by a pulsed current through a small coil inside the body of a special bi-directional, electromagnetic, ellipsoidal sensor of the size  $11 \times 33 \text{ mm}$ . The accuracy of the measurement of velocity is  $\pm 0.01 \text{ m/s}$ . This device was mounted on a special moving trolley with a water level indicator. The velocity meter was connected via a converter-amplifier to the IBM compatible computer where the relevant time series were recorded.

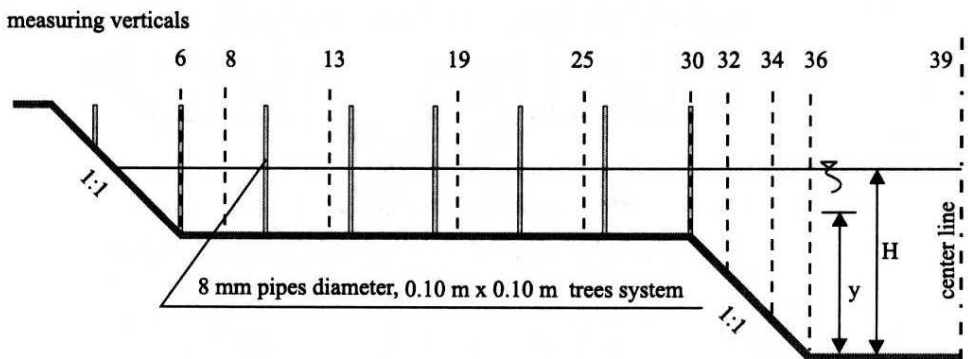


Fig. 2. Arrangements of trees in respect to measuring verticals in test 3

The measurements of instantaneous longitudinal velocities were carried out at 48 points at 10 verticals. The position of the verticals is shown in Fig. 1. In Fig. 2 one can see how these verticals were positioned in respect of the "trees" in the third experiment. The time of velocity recording at each point was roughly 40

min and the sampling interval of 0.2 s was taken. It turned out that a time slightly shorter than 27 min was enough to obtain fully steady statistical characteristics of the flow and therefore the time series of 8000 elements (corresponding to a time period of about 26.7 mins) were further elaborated. Exemplary three-minute intervals of time series of streamwise instantaneous velocities for a selected measuring point are given in Fig. 3. Three various series were obtained during the three tests described above. The measured velocity field was obviously of a stochastic nature and the stationarity and ergodicity of the process was checked. It is important to note that sporadic abrupt spikes appearing in velocity time series were removed to avoid their significant influence on the variance and further statistical moments. Spikes that were removed exceeded three values of standard deviation of the unaltered measurements and they were replaced by the mean values of five neighbouring values. Fortunately the number of spikes was small enough and sophisticated methods of their detection and replacement could be avoided. One can find information on various methods of despiking the data in Goring and Nikora (2002).

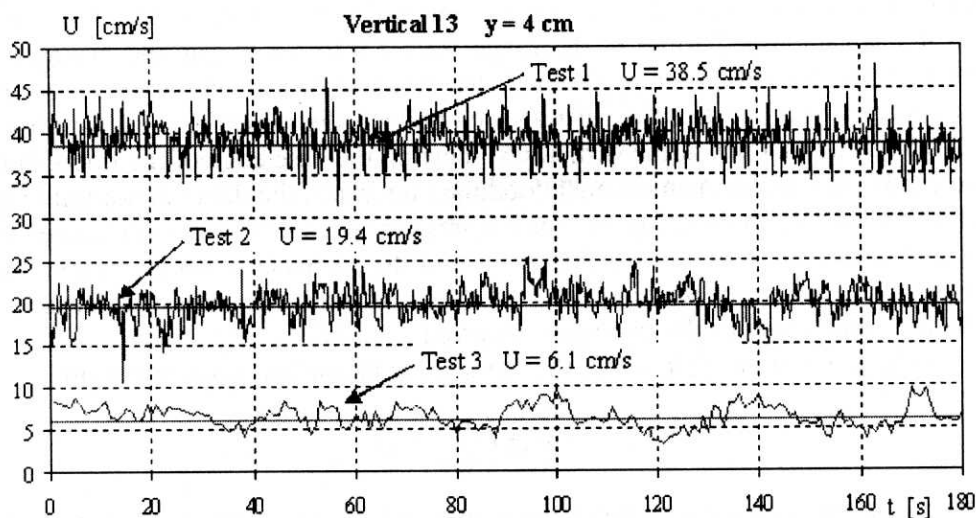


Fig. 3. Examples of time series of streamwise velocities – three tests. The sampling rate is 2.5 Hz

### 3. Overview of the Flow Field

One of the main concerns in the studies of compound channel flows is the behaviour of local time-mean velocities. Their knowledge is also crucial in the recognition of the turbulence properties, which is the main aim of this study. The detailed studies of mean velocities in the described channel were performed earlier

in (Kubrak and Żbikowski 1995) where the isovels were presented for smooth and rough floodplain beds. The velocity field in a two-stage channel is obviously three dimensional (Knight et al. 1994), nevertheless distributions of longitudinal velocities  $U$  give us some insight into the flow structure in such channels. Besides, in the areas where the log-law distributions at a vertical are satisfied, the values of longitudinal time-mean velocities allow us to obtain local friction velocities  $U_*$  and consequently the bed shear stress from the relationship  $\tau = \Delta U_*^2$ . Both these parameters are extremely important as normalising parameters for various turbulent characteristics, as well as e.g. for the quantitative description of sediment transport.

It is expected that in case of the smooth channel the vertical distribution of the mean-time longitudinal velocities in the inner region  $y/h < 0.2$  should agree with the equation (e.g. Prandtl 1956):

$$U^+ = \frac{1}{\kappa} \ln(y^+) + A, \quad (1)$$

where  $U^+ = U/U_*$ ,  $y^+ = yU_*/\nu$ ,  $\nu$  – distance from the bed,  $\nu$  – kinematic viscosity of water,  $\kappa$  – universal von Karman constant ( $\kappa = 0.41$ ),  $A$  – integral constant. Regardless of the Reynolds number, the integral constant should be the same and it was established to be in the range from 5.0 to 5.3 (Nezu and Nakagawa 1993) although some authors obtained that value from a much larger range. In our experiment at most of the verticals we obtained the values of  $A$  ranging from 5.2 to 5.5 (Fig. 4). Only at the verticals 6 – beyond the base edge of the floodplain, and 32, 34, 36 – at the main channel/floodplain interface, the data did not fulfil Eq. (1). Large deviations from logarithmic law in these areas are most likely caused by three-dimensional nature of the flow there and the particularly strong momentum transport in the spanwise direction. At these verticals the largest decrease of velocity values close to the bed were observed.

In the wall region,  $y/h < 0.2$ , the log-law for rough bed takes the form:

$$U^+ = \frac{1}{\kappa} \ln\left(\frac{y}{k_s}\right) + A_r, \quad (2)$$

where  $k_s$  is the equivalent granular roughness and for a completely rough wall  $A_r$  is considered as universal constant equal to 8.5. The value of the parameter  $k_s$  may be determined from the distribution of mean velocity in the region where it satisfies the log-law (2).

Much larger differences between the values of velocities in the main channel and in the floodplains are observed when the floodplains are covered with the rough bed. It may be a reason of the creation of considerable shear forces caused by large lateral gradients of water velocities. The log-law is again violated in the intermediate region while it is satisfactorily fulfilled in both the main channel and rough floodplains (Fig. 5). The equivalent granular roughness varied from

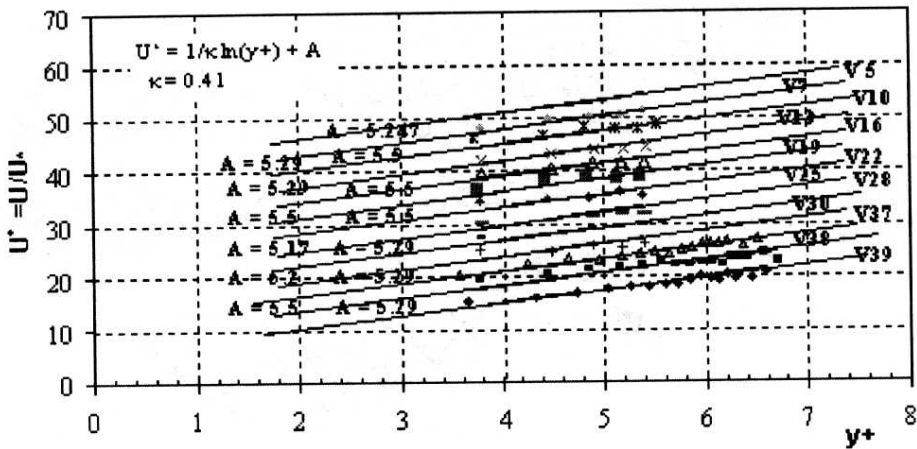


Fig. 4. Comparison of measured mean velocity distributions with a log-law for hydraulically smooth bed

the value of almost 10 mm in the centre of rough floodplains to 0.19 mm in the centre of main channel.

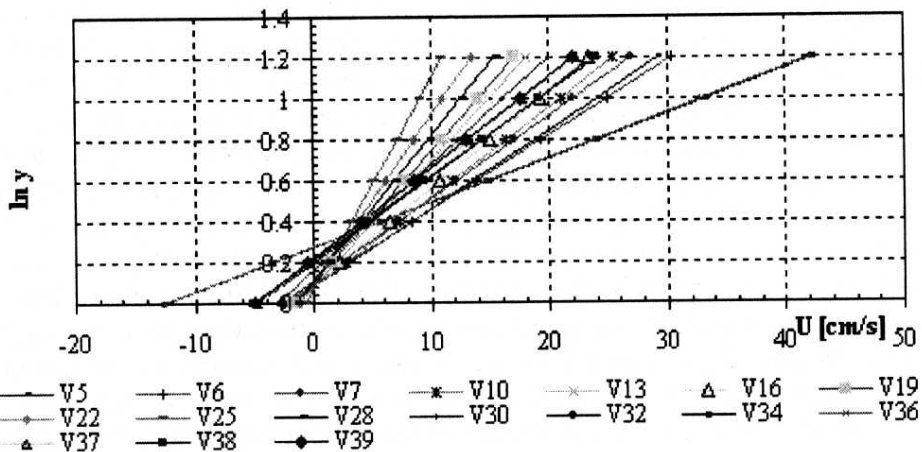


Fig. 5. Comparison of measured mean velocity distributions with a log-law for hydraulically rough bed

Having the slopes of the corresponding straight lines fulfilling Eqs. (1) and (2) it is easy to find values of local friction velocities  $U_*$  and consequently the local shear stresses  $\tau$  as  $\tau = \rho U_*^2$ . The authors caution that the standard error in such estimates of  $U_*$  may be quite large (Wilcock 1996). Fig. 6 presents the distributions of friction velocity and the local shear stresses at the measuring cross-section for both smooth and rough channel. The values of  $U_*$  and  $\tau$  at the verticals where the log-laws (1) and (2) are violated, may be treated as only of an

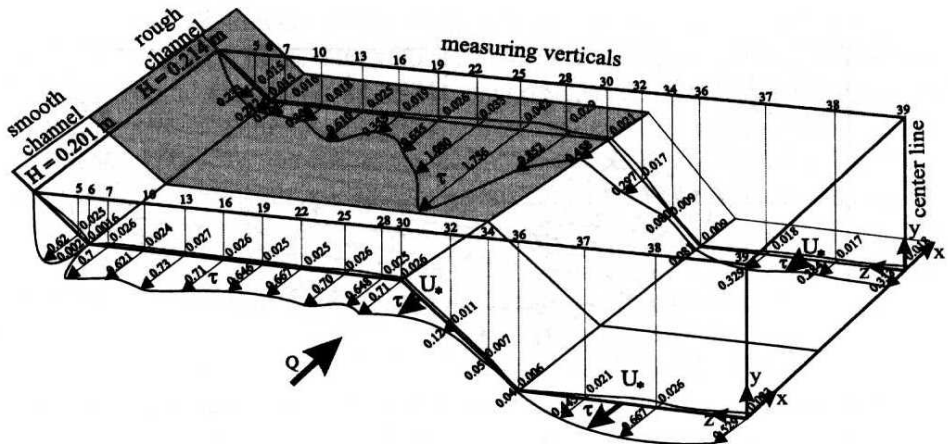


Fig. 6. Distributions of bed shear stress  $\tau$  and friction velocities  $U_*$  in a compound channel with smooth and rough floodplains

indicatory character. Unfortunately it was not possible to measure shear stresses directly with the Preston tube during the experiment. It is worth mentioning that in the central parts of the main channel and floodplains, the values of friction velocity are in close agreement with the overall value obtained from the formula  $U_* = \sqrt{Rgi}$  ( $R$  – hydraulic radius,  $i$  – bed slope) and the differences with the local values didn't exceed 10%. Fig. 6 reveals high increase of the bed shear stress at the vertical 25 especially in case of rough floodplains. It is most probably caused by the existence of high lateral shear stresses in that area where the momentum transport in the lateral direction is probably most considerable. It is an effect of the boundary equilibrium condition assuming the proportionality of the bed shear  $\tau$  to the sum  $\tau_{yb} + s\tau_{zb}$ , where  $\tau_{yb}$  and  $\tau_{zb}$  are vertical and lateral Reynolds stresses at the bed and  $s$  is the side channel slope (Knight and Shiono 1990). The bed shear stress is a very sensitive parameter and the perturbations in its distribution around the wetted parameter revealed in Fig. 6 may possibly be explained by the existence of secondary flow cells, as was the case in other experimental work (Knight et al. 1994). Local shear stresses in the present experiments varied in the first test (smooth channel) in the range of from 0.45 N/m<sup>2</sup> in the main channel to 0.73 N/m<sup>2</sup> over the floodplains and from 0.21 N/m<sup>2</sup> to 1.76 N/m<sup>2</sup> respectively in the second test (rough channel). It is a well known fact that a large part of the turbulence is generated at the bed and the distribution of bed shear stresses should somehow be reflected in the distributions of basic turbulence characteristics. This problem will be discussed later.

It was found that in the case of the occurrence of high vegetation on floodplains, the values of velocities are fairly uniformly distributed along verticals and the log-law is not satisfied. Therefore, another method of the describing vertical velocities and consequently in such case, shear stresses have to be applied. A new



approach for the determination of vertical distributions of mean velocities in vegetated channels has recently been proposed and tested against the considered data by Rowiński and Kubrak (2002a, b). It is also worth mentioning that a large amount of information in respect to the mean flow field is contained in the spanwise distribution of depth-averaged longitudinal velocities in compound channels. This problem has also been studied in respect of the considered compound channel in (Kubrak and Rowiński 2001).

#### 4. Turbulence Structure

One of the most important characteristics of turbulent flow is its one-dimensional intensity  $\sqrt{u'^2}$ , where  $u'$  is the fluctuating component in the Reynolds decomposition of the instantaneous point velocity  $u$  ( $u = U + u'$ ). In case of stationary turbulent flows (when statistical parameters related to the flow do not change with time) the time average for any quantity  $\xi$  is:

$$\bar{\xi} = \frac{1}{2T} \int_{-T}^T \xi dt \quad (3)$$

at a given point. The sampling time  $2T$  should be sufficiently large compared to the time scale of small eddies and small compared to time scales of large eddies. The turbulent intensity represents quite a large part of the total turbulence kinetic energy  $k$  and thus is very informative; its contribution in the kinetic energy of turbulence ranges between 45% to 80 % (McLean and Smith 1979, Nezu and Nakagawa 1993, Sukhodolov and Rhoads 2001). Since the estimates of friction velocity  $U_*$  are crude, we will discuss the behavior of the relative turbulence intensity  $\sigma = \sqrt{u'^2}/U$  utilizing mean-time velocities for normalization. These values can be considered as being much more accurate than  $\sigma/U_*$ . It has also been shown recently that even if the friction velocity is determined relatively accurately, the normalization of the root-mean-square deviation of the longitudinal velocity  $\sigma$  on the friction velocity is not as successful in the statistical sense, as using the local mean velocity (Nikora and Smart 1997). The search for the vertical distributions of the turbulence intensity is one of preliminary tasks for the investigators. Nikora and Smart (1997) have shown that the turbulence intensity depends not only on the relative distance from the bottom (as assumed by Nezu and Nakagawa 1993), but also on the corresponding turbulence scale (external scale of the inertial region described in the sequel). Fig. 7 presents distributions of the relative intensity of turbulence along all selected verticals. In most cases  $\sigma$  increases towards the channel bottom. Only once in the third test (with high vegetation) can we observe the decrease of this value at the vertical 32 placed on the slope between the main channel and the floodplain. In some cases one can observe some increase

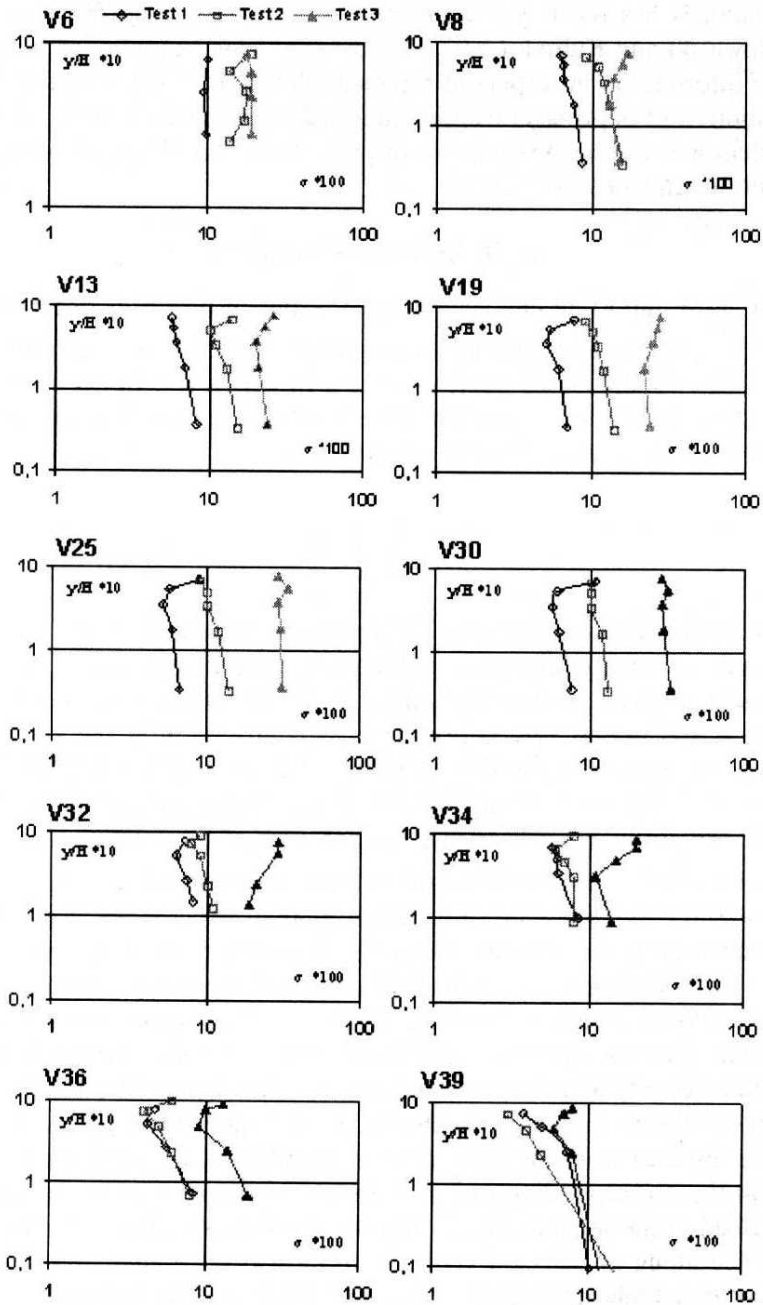
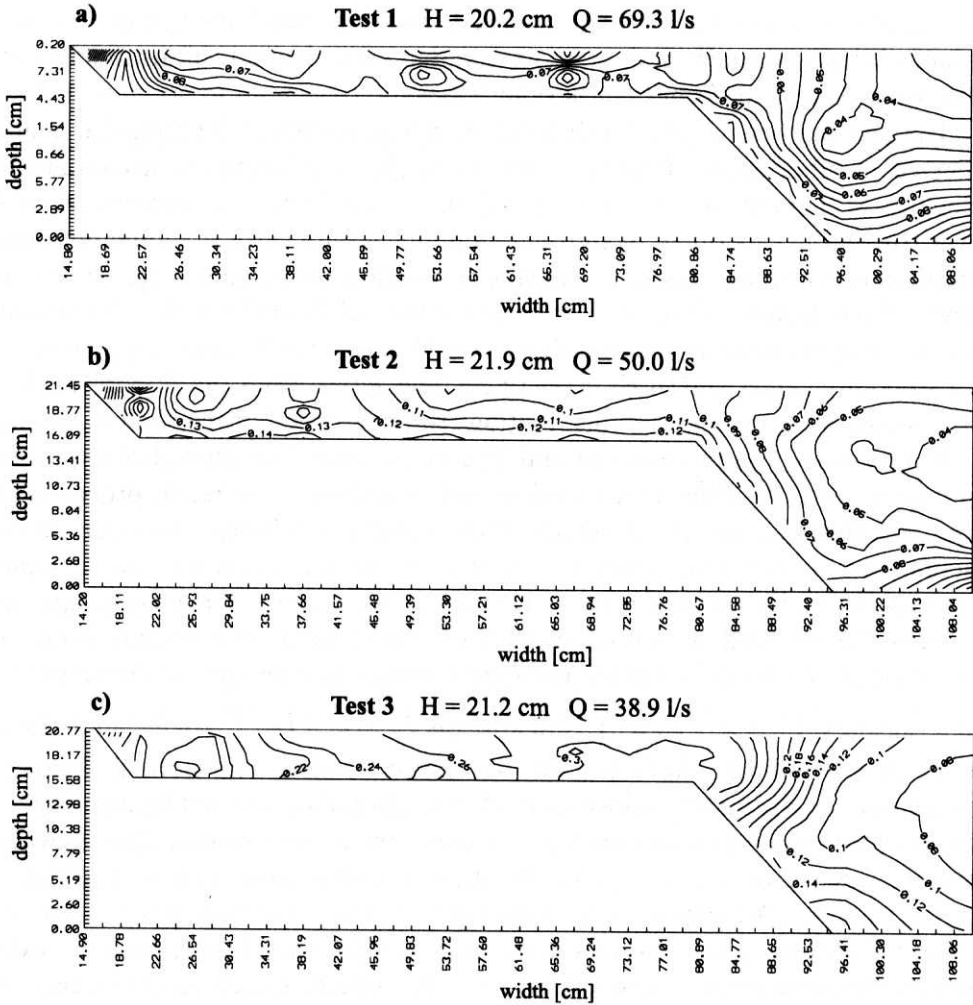


Fig. 7. Vertical distributions of relative turbulence intensity



**Fig. 8.** Contour lines for relative turbulent intensities in a compound channel  
 a) smooth bed, b) rough floodplains, c) rough floodplains covered with trees

of parameter  $\sigma$  from a certain minimum value towards the water surface. It may be caused by additional generation of turbulence by the air-water interface. The general pattern in the distributions of relative turbulence intensity is shown in Fig. 8 in which contour lines of  $\sigma$  are shown. One can observe that the intensity of turbulence increases considerably as the (granular) roughness size increases, which is evident on the floodplain where the roughness was changed. The changes of roughness on the floodplains do not influence the intensity of turbulence at the central vertical of the main channel. It is clear that the high vegetation generates turbulence along whole verticals by creating a wake behind a row of parallel rods. In other words, some large local gradients of mean velocity exist behind

the "trees". It makes the relative turbulence intensity much greater in the third variant of the experiment and, moreover, in that case, the vertical distributions of intensity are more uniform than in other cases.

The unusual behaviour of turbulence in channels with high vegetation is also reflected in other terms. While in a few cases the distributions of instantaneous velocities at a point may be represented by almost Gaussian distribution, it is never true in the experiment with rough floodplains with vertical aluminium pipes placed on them. It was checked by means of standard statistical chi-square test. To a level of significance of 0.05 we can disprove the null hypothesis that the instantaneous velocities have normal distribution in 45 cases over 52 analysed time series in a smooth channel and in 41 cases of 50 time series when the floodplains had rough beds. Most of Gaussian distributions were recorded in the shallow section of the channel – 6 in the first test and 7 in the second. The above has important consequences at the elementary level of understanding of turbulent processes. A silent assumption about the adequacy of the normal distribution in respect of the fluctuating velocities time series is very often made and as shown, such assumption may be readily violated. One may suspect that the non-Gaussian properties may also be revealed in natural conditions. This fact is also evident from the distributions of normalized third and fourth statistical moments, or consequently from skewness  $C_s = \overline{u'^3} / (\sqrt{\overline{u'^2}})^3$  and kurtosis  $E_s = \overline{u'^4} / (\overline{u'^2})^2$  coefficients. These values clearly indicate that we could not expect to deal with normal Gaussian distributions of fluctuating velocities neither in the points affected by high vegetation or those situated above the sloping bank of the deeper section. The skewness characterizes the degree of asymmetry of the instantaneous velocity distribution around its mean. A positive value of skewness signifies distribution with an asymmetric tail extending out towards more positive values whereas a negative value signifies the occurrence of this tail on the other side of the distribution. In most cases the skewness coefficient is positive near the bed and negative at a distance from both the bed and water surface. Similar results are also observed in natural river flows (e.g. Nikora and Smart 1997). Some deviations from this rule are observed when we deal with the third variant of the experiment (with high vegetation) and in the main channel/floodplains interface. In these particular locations, generation of additional turbulence by created wakes or lateral velocity gradient may cause transport of excess turbulent energy downwards to the bottom. Otherwise, we have a typical situation of the transport of turbulent energy in a direction toward the channel bed (skewness is negative in these points). The greatest variation in the range of velocity fluctuations (degree of turbulent energy pulsation) is also observed for the flow when high vegetation is situated in the shallow parts of the channel and is revealed by the largest variation of kurtosis. In most cases the values of kurtosis are negative, hence distributions of instantaneous velocities are usually platykurtic.

One of the main concerns in turbulence studies is the estimate of temporal and, if possible, spatial characteristics of existing eddies in the flow. Possibly the easiest is the evaluation of the macro time-scale of turbulence defined with the use of the autocorrelation function with the time shift  $\tau$ :  $R(\tau) = \lim_{T \rightarrow \infty} \frac{1}{2T} \int_{-T}^T u'(t + \tau)u'(t)dt$ .

This is

$$T_E = \int_0^{\infty} R(\tau)d\tau. \quad (4)$$

The autocorrelation functions of the longitudinal velocities exhibit similar forms for all points and variants of the experiment. They assume the shape of decaying curves and from a certain point to be an alternation of the domains of the positive and the negative values is evident. Typical graphs representing  $R(\tau)$  can easily be found in the literature (e.g. Nezu and Nakagawa 1993). The characteristic point mentioned determines the time scale of turbulence  $T_E$  which varies greatly:

- over floodplains: with smooth beds – from 0.27 s to 0.62 s; with rough beds – from 0.25 s to 0.83 s and with high vegetation – from 0.35 s to 0.97 s;
- in the main channel – from 0.37 s to 1.97 s, 0.23 s to 0.76 s and 0.5 s to 0.82 s in three variants of the experiment respectively.

The transformation from temporal characteristics of the signals to the spatial characteristics can be made by means of the Taylor hypothesis of “frozen turbulence” which is applicable if the intensity of turbulence of flow and change in the average velocity are small. In our experiments the values of  $\sigma/U$  only in a few cases above beds with high vegetation were as high as 0.3, but in most cases these values were small enough to confirm the justness of the Taylor hypothesis.

Thus the Eulerian integral scale (the measure of the longest correlation distance in longitudinal direction or considerable energy containing eddies) may be evaluated as equal to  $L_E = UT_E$ . A characteristic feature of the mean longitudinal sizes of the largest eddies in the shallow sections of the channel is that they achieve the lowest values in the test with high vegetation varying in the range of from  $0.4H$  to  $2.1H$  ( $H$  – water depth) and the largest ones over smooth beds (from  $1.8H$  to  $3.2H$ ) (see Fig. 9). Evidently physical obstacles set back the increase of longitudinal “macro-eddies”. This property is not observed in the main channel and the roughness of floodplains does not influence the growth of longitudinal eddies very much there. Only at a few points (for example at a centre line) do these values exceed  $2H$ . The lowest values of  $L_E$  are usually achieved at points close to the bed and (when measured) close to the water surface. The estimated Eulerian integral scales are commensurable with other observations in laboratory flows (see for example Czernuszenko and Lebiecki 1980).

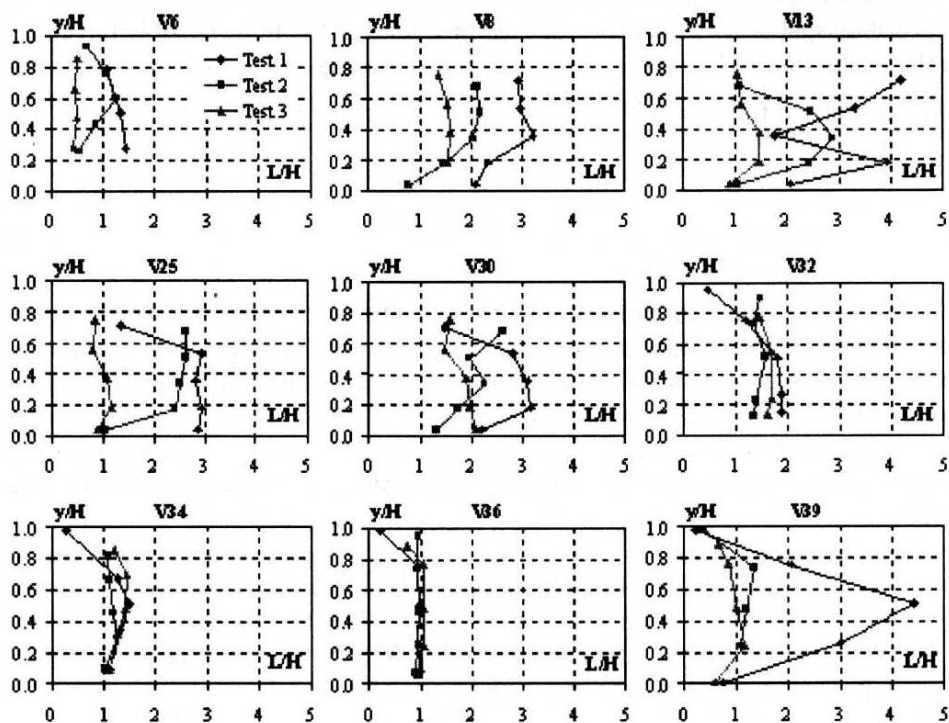


Fig. 9. Vertical distributions of longitudinal macro-eddies

Having known the autocorrelation function  $R(\tau)$  and assuming that this function is related to the Lagrangian autocorrelation function  $R^L(\tau)$  for the sequence of velocity of selected liquid element by means of expression  $R^L(\beta\tau) = R(\tau)$  ( $\beta$  – a dimensionless coefficient), one may evaluate the turbulent diffusion coefficient in the longitudinal direction at a given point with the use of equation (Engelund 1969, Pasquill 1962):

$$K = U \frac{\sqrt{u'^2}}{2.5} T_E. \quad (5)$$

This quantity is extremely important to evaluate the capabilities of the turbulent stream to transfer mass, momentum and heat in the longitudinal direction (e.g. Rowiński 2001). Considering only the shallow part of the channel it is evident that this coefficient assumes the largest values when the bed is smooth (from 26  $\text{cm}^2/\text{s}$  to 58  $\text{cm}^2/\text{s}$ ) and the smallest when the floodplains are vegetated (from 1 to 12  $\text{cm}^2/\text{s}$ ). It is quite interesting that this coefficient becomes largest above the sloping bank of the deeper section in the third variant of the experiment. It is caused by particularly large lateral gradients in a longitudinal direction and consequently large intensity of turbulence. In the centerline of the main channel,

the bed roughness in the shallow section does not influence the value of diffusion coefficient  $K$  very much. The above evaluations of coefficient  $K$  may be treated as being of a qualitative character only, as Eq. (5) was not proved to be valid for analogous experiments. Complex interplay among the different processes may lead to a fundamentally different proportionality factor  $\beta$  and moreover, it could lead to a completely different relationship than (5). It is of great interest to examine in depth the derivation of the expression for  $K$  in such cases or to plan a special series of experiments allowing for the direct measurements of the diffusion coefficient in a compound channel.

Great efforts have been made towards an understanding of small-scale turbulent velocity fluctuations, which are assumed to be stationary, homogeneous and isotropic in the statistical sense. For large Reynolds numbers these fluctuations are supposed to exhibit universal behaviour on scales smaller than the integral one. One method of analysis of isotropic (locally) turbulence is the study of correlation coefficients as described above. Another method is to analyse velocity fluctuations in terms of their spectrum in much the same way as a beam of light can be separated into its spectral components. The turbulence consists of superposition of eddies of various sizes; large size eddies cause fluctuations of low frequency, whereas smaller eddies cause fluctuations of high frequency. Each eddy has a certain kinetic energy which is determined by its velocity or corresponding frequency (Garde 1994). According to the original Kolmogorov concept velocity spectra consist of three ranges: the production range, where spectral behaviour has not been identified specifically, the inertial subrange where spectra follow the “ $-5/3$ ” law (there is no energy production or dissipation in this subrange) and the viscous range where spectra decay much faster than in the inertial subrange due to dissipation (Nikora 1999). Recently Nikora (1999) proposed an explanation for the existence of the regions in which an inverse ( $-1$ ) power law is fulfilled. Taking into account the results of the theory of locally isotropic turbulence developed by Kolmogorov, one may claim that the influence of the large-scale on the fine-scale fluctuations may be described by two parameters: the rate of energy dissipation  $\varepsilon$  and the integral scale  $L$  (Praskovsky 1991). To estimate the rate of energy dissipation we have to demonstrate the existence of the local isotropy of turbulence and find the inertial interval for which the spectral function satisfies the well-known Kolmogorov  $-5/3$  power law or the structure function satisfies the  $2/3$  law. The detailed analysis of spectral function and the search of frequencies and wave numbers at which the average flow of energy from the large-scale to the fine-scale fluctuation, provide important information on the turbulence structure. The results presented below are based upon frequency spectra only since this method seems to be more accurate than the use of the structure functions. Efforts are directed towards the search of the range of frequencies for which the following relation is valid:

$$S(\omega) = \frac{1}{\pi} \int_0^{\infty} \cos(\omega, t) R(t) dt = C_K (\varepsilon U)^{2/3} \omega^{-5/3}, \quad (6)$$

where  $C_K$  is Kolmogorov's constant (usually taken as equal to 0.48),  $\varepsilon$  – dissipation rate of turbulent energy,  $\omega$  – the circular frequency,  $\omega = 2\pi f$ . The existence of the inertial subrange in the velocity spectrum is expected if a sufficiently large Reynolds number characterizes the investigated flow.

Time series with the removed spikes as described in the previous section were used in the analyses. Unfortunately, relationship (6) is not fulfilled at every point of the considered compound channel. The best conformity was found at the central verticals of both shallow and deep sections of the channel. Examples of spectral distributions are shown in Fig. 10. One can see that Kolmogorov's “ $-5/3$ ” power law is satisfied in relatively narrow ranges of frequencies. The important disadvantage of the apparatus used is revealed by those spectra, which is manifested in the appearance of white noise at relatively low frequencies (in the case of vegetated channels even as low as 1 Hz). The lower decrease of the spectra and the observed maxima at low frequencies in the case of vegetated floodplains point to the additional energy supply except for the energy cascade. This confirms the result obtained by Nezu and Onitsuka (2001). These authors explain this energy supply by the existence of wake vortices generated behind all vegetation rods and by the coherent vortices. This explanation seems to be rational, but cannot be confirmed by direct observations in one-dimensional measurements.

At the points where Eq. (6) holds, the dissipation rate  $\varepsilon$  was evaluated. When considering the shallow part of the channel, one can observe that the dissipation rate ranges from  $5.8 \text{ cm}^2/\text{s}^3$  to  $32.5 \text{ cm}^2/\text{s}^3$  above the smooth bed, from  $7.8 \text{ cm}^2/\text{s}^3$  to  $17.9 \text{ cm}^2/\text{s}^3$  when the bed is rough and from  $3.1 \text{ cm}^2/\text{s}^3$  to  $4.8 \text{ cm}^2/\text{s}^3$  above the vegetated floodplains. Too few data are available to derive any profound conclusions in respect of the distributions of the dissipation rate in relation to depth. One important observation is that the roughness has less effect upon the dissipation rate than on the turbulence intensity and the macroscale, which conforms with the findings of other researchers (Nezu and Nakagawa 1993).

Knowing the dissipation rate  $\varepsilon$  one can easily evaluate the Kolmogorov microscale  $\eta$  characterizing the sizes of dissipative eddies as  $\eta = (v^3/\varepsilon)^{1/4}$  where  $v$  is the kinematic viscosity of the fluid. It was stated that microscale eddies are not so much affected by bed roughness (which is the result of the earlier statement in respect of dissipation rate) and the largest differences in the values of  $\eta$  exceed 60% between flows in the smooth and vegetated channel, but these values are usually very close to each other. The sizes of dissipative eddies range from 0.013 cm to 0.020 cm on both smooth and rough floodplains and from 0.01 cm to 0.024 cm when vegetation occurred. In the main channel those eddies are slightly larger and their size vary from 0.014 cm to 0.031 cm. It is worth pointing out that



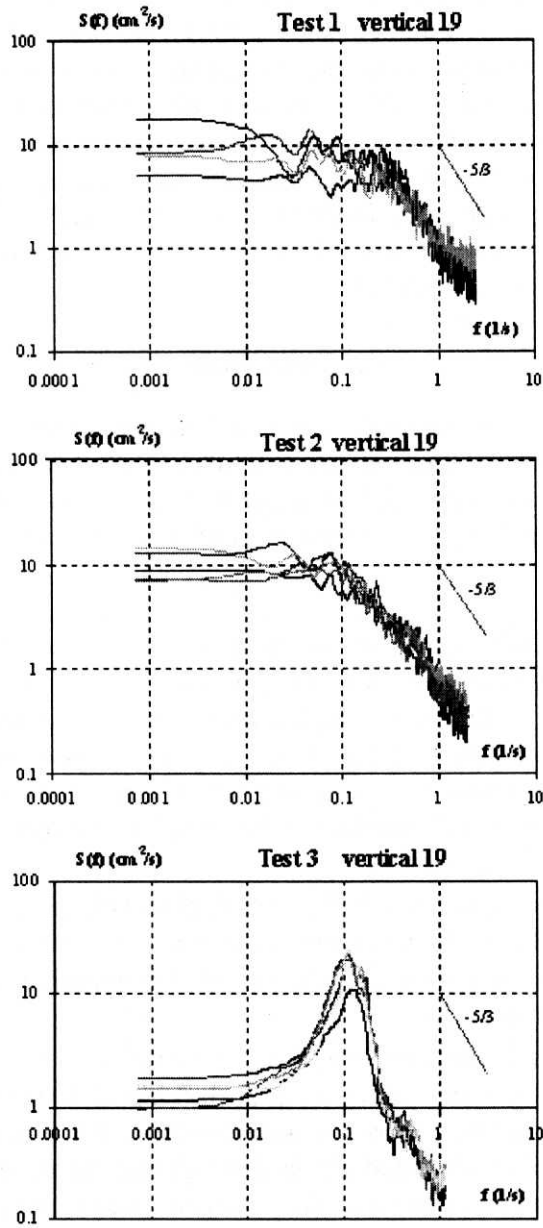


Fig. 10. Power spectra at a selected vertical (center of the floodplain) at three different roughness conditions

other turbulent scales can also be considered. A well-known Taylor microscale  $\lambda$  is composed of a macroscale velocity  $u'$  and the inherently inner variables  $\nu$  and  $\varepsilon$ , but since it has much worse physical interpretation we will not evaluate its value in the present study (Nezu and Nakagawa 1993). An interesting characteristic is an upper boundary of the inertial subrange of the velocity spectrum recently discussed by Nikora and Smart (1997). To have less uncertainty in its derivation, a much broader frequency range should be taken into account, but this calls for the use of other apparatus. New measurements are currently carried out with the use of two-component Acoustic Doppler Velocimeter ADV, which hopefully will allow us to fill in the gaps in the information concerning turbulent structure in the compound channel considered.

## 5. Conclusions

The results of the present paper are based on the measurements of instantaneous velocities in a two-stage trapezoidal channel under three various roughness conditions on the floodplains (smooth bed, rough bed in overbank channels and rough overbank channels with high vegetation placed). These results can be summarized as follows:

1. The vertical distributions of the local mean velocity can be satisfactorily described by logarithmic laws in the two first variants of the experiment in the main channel and in the shallow part of it. The logarithmic law does not apply above the sloping bank of the deeper section of the channel as well as in the experiment with high vegetation situated on the floodplains. In the situation with high vegetation occurring in overbank channels another model should be applied.
2. Where the logarithmic law applies, the friction velocity and shear stress may be evaluated. In the central parts of the main channel and floodplains these values are in close agreement with the overall quantities obtained from the uniform flow formula.
3. The longitudinal turbulence intensity variations in relation to depth are typical, i.e. the greatest values occur at the channel bottom and the smallest at some short distance from the water surface. The intensity of turbulence increases significantly when the bed roughness increases and also at the interface between shallow and deep areas of the channel.
4. Longitudinal sizes of the largest eddies were estimated by means of autocorrelation functions and the hypothesis of "frozen turbulence". It was shown that in the floodplains these sizes are smallest in the test with high vegetation ( $0.4H$  to  $2.1H$ ) and largest when the bed was smooth there ( $1.8H$  to  $3.2H$ ).

5. At some points, the investigated spectral functions were characterized by the existence of an inertial subrange. They satisfied the Kolmogorov “ $-5/3$ ” power law, which allowed for the use of the results of the theory of locally isotropic turbulence. In the case of the vegetated channel, an additional energy supply apart from the energy cascade is observed at low frequencies, which conforms with the findings of other authors.
6. The values of the turbulent energy dissipation obtained from the Kolmogorov theory vary in the range of between 3 to 32 cm<sup>2</sup>/s<sup>3</sup>.
7. Kolmogorov microscales are not significantly affected by bed roughness and vary from 0.01 cm to 0.03 cm.

The results of the present paper clearly indicate that it is worth while conducting detailed measurements of the turbulence structure by means of more sensitive testing equipment operating at higher frequencies and also allowing for estimates of other velocity components. Such experiments are carried out in the same laboratory and the results will be reported shortly.

#### Acknowledgements

The present paper is the result of a collaborative work for which funding was sponsored by two grants from the Polish Committee for Scientific Research, Nos. 6P04D02020 and 6P06H04320.

#### References

- Barua D. K., Rahman K.H. (1998), Some aspects of turbulent flow structure in large alluvial rivers, *Journal of Hydraulic Research*, Vol. 36, No. 2, 235–252.
- Czernuszenko W., Lebiecki P. (1980), Turbulent characteristics of stream in open channel, *Archiwum Hydrotechniki*, Vol. 27, 1, 19–38.
- Dinehart R. L. (1999), Correlative velocity fluctuations over a gravel river bed, *Water Resources Research*, Vol. 35, No. 2, 569–582.
- Engelund F. (1969), Dispersion of floating particles in uniform channel flow, *Journal of Hydraulic Division*, ASCE, Vol. 95, No. HY4.
- Garde R. J. (1994), *Turbulent flow*, Wiley & Sons, New York, p. 287.
- Goring D. G., Nikora V. I. (2002), Despiking acoustic Doppler velocimeter data, *Journal of Hydraulic Engineering*, Vol. 128, No. 1, 117–126.
- Knight D. W., Brown F. A. (2000), Resistance studies of overbank flow in rivers with sediment using the flood channel facility, *Journal of Hydraulic Research*, Vol. 39, No. 3, 283–301.
- Knight D. W., Shiono K. (1990), Turbulence Measurements in a Shear Layer Region of a Compound Channel, *Journal of Hydraulic Research*, Vol. 28, No. 2, 175–195.

- Knight D. W., Yuen K. W. H., Al-Hamid A. A. I. (1994), *Boundary Shear Stress Distributions in Open Channel Flow, Mixing and Transport in the Environment*, Eds. K. J. Beven, P. C. Chatwin and J. H. Millbank, John Wiley & Sons, 51–87.
- Kubrak J. (1999), Friction factors in channel with compound cross-section, *Proc. 19th Polish Hydraulics School*, Frombork, 69–74 (in Polish).
- Kubrak J., Rowiński P. M. (2001), Velocity and discharge prediction in straight compound channels using the eddy viscosity concept, *Proc. 21st Polish Hydraulics School*, Sasino, 61–66 (in Polish).
- Kubrak J., Żbikowski A. (1995), Investigation into the Hydraulic Characteristics of Channels with Flood Plains, *Archives of Hydro-Engineering and Environmental Mechanics*, Vol. 43, No. 3–4, 31–37.
- McLean S. R., Smith J. D. (1979), Turbulence measurements in the boundary layer over a sand wave field, *Journal of Geophysical Research*, Vol. 84, No. 12, 7791–7808.
- Myers W. R. C., Lyness J. F., Cassells J. (2000), Influence of boundary roughness on velocity and discharge in compound river channels, *Journal of Hydraulic Research*, Vol. 39, No. 3, 311–319.
- Nepf H. M. (1999), Drag, turbulence, and diffusion in flow through emergent vegetation, *Water Resources Research*, Vol. 35, No. 2, 479–489.
- Nepf H. M., Vivoni E. R. (2000), Flow structure in depth-limited, vegetated flow, *Journal of Geophysical Research*, Vol. 105, No. C12, 28547–28557.
- Nezu I., Nakagawa H. (1993), *Turbulence in Open-channel Flows*, IAHR Monograph, Balkema, Rotterdam, p. 281.
- Nezu I., Onitsuka K. (2001), Turbulent structures in partly vegetated open-channel flows with LDA and PIV measurements, *Journal of Hydraulic Research*, Vol. 39, No. 6, 629–642.
- Nikora (1999), Origin of the “–1” spectral law in wall-bounded turbulence, *Physical Review Letters*, Vol. 83, No. 4, 734–736.
- Nikora V. I., Rowiński P. M., Sukhodolov A., Krasuski D. (1994), Structure of River Turbulence Behind Warm Water Discharge, *Journal of Hydraulic Engineering*, Vol. 120, No. 2, 191–208.
- Nikora V. I., Smart G. M. (1997), Turbulence Characteristics of New Zealand Gravel-Bed Rivers, *Journal of Hydraulic Engineering*, Vol. 123, No. 9, 764–773.
- Pasquill F. (1962), *Atmospheric Diffusion*, Van Nostrand, London.
- Prandtl L. (1956), *Flow dynamics (Dynamika przepływów)*, Warszawa, PWN (Polish translation).
- Praskovsky A. A. (1991), Local Structure of Turbulence in Flows with Large Reynolds Numbers, *Chaos*, Vol. 1, No. 2, 37–241.

- Rowiński P. M. (2001), *Constituent transport*, to be published in Encyclopedia of Life Support Systems, UNESCO, EOLSS Publishers Co.
- Rowiński P. M., Czernuszenko W., Koziół A., Kuśmierczuk K., Kubrak J. (1998), Longitudinal Turbulence Characteristics in a Compound Channel under Various Roughness Conditions, *3<sup>d</sup> International Conference on Hydroscience and Engineering*, Cottbus/Berlin, <http://www.bauinf.tucottbus.de/ICHE98/proceedings>.
- Rowiński P. M., Czernuszenko W. (1998), Experimental study of river turbulence under unsteady conditions, *Acta Geophysica Polonica*, Vol. XLVI, No. 4, 462–480.
- Rowiński P. M., Czernuszenko W., Pretre J. M. (2000), Time-dependent shear velocities in channel routing, *Hydrological Sciences Journal*, Vol. 45, No. 6, 881–895.
- Rowiński P. M., Kubrak J. (2002a), A mixing-length model for predicting vertical velocity distribution in flows through emergent vegetation, accepted for publication, *Hydrological Sciences Journal*.
- Rowiński P. M., Kubrak J. (2002b), Velocity profiles on vegetated flood plains, in: *Velocity profiles on vegetated flood plains*, River Flow 2002, D. Bousmar, Y. Zech (eds.), 2002 Sweets & Zeitlinger, Lisse, The Netherlands, Vol. 1, 303–309.
- Shiono K., Knight D. W. (1991), Turbulent open channel flows with variable depth across the channel, *Journal of Fluid Mechanics*, Vol. 222, 617–646.
- Smart G. M. (1999), Turbulent velocity profiles and boundary shear in gravel bed rivers, *Journal of Hydraulic Engineering*, Vol. 125, No. 2, 106–116.
- Sofialdis D., Prinos P. (1999), Turbulent flow in open channels with smooth and rough flood plains, *Journal of Hydraulic Research*, Vol. 37, No. 5, 615–640.
- Sukhodolov A. N., Rhoads B. L. (2001), Field investigations of three-dimensional flow structure at stream confluences, 2, Turbulence, *Water Resources Research*, Vol. 37, No. 9, 2411–2424.
- Tominaga A., Nezu I. (1991), Turbulent Structure in Compound Open-Channel Flows, *Journal of Hydraulic Engineering*, Vol. 117, No. 1, 21–41.
- Wilcock P. R. (1996), Estimating Local Bed Shear Stress from Velocity Observations, *Water Resources Research*, Vol. 32, No. 11, 3361–3366.